PHYSICO-CHEMICAL BASICS OF METALLURGICAL PROCESSES / **ФИЗИКО-ХИМИЧЕСКИЕ ОСНОВЫ МЕТАЛЛУРГИЧЕСКИХ ПРОЦЕССОВ**

UDC 669.71
DOI 10.17073/0368-0797-2023-4-459-470

Original article
Оригинальная статья

Thermodynamic assessment of conditions for co-reduction of zinc and iron by carbon from oxides of concentrates and waste from metallurgical enterprises

N. F. Yakushevich, E. V. Protopopov, M. V. Temlyantsev, I. V. Strokina

Siberian State Industrial University (42 Kirova Str., Novokuznetsk, Kemerovo Region – Kuzbass 654007, Russian Federation)

protopopov@sibsiu.ru

Abstract. The paper considers theoretical issues of reduction of zinc and iron by carbon from oxides of concentrates and zinc-containing metallurgical waste (dust and sludge of metallurgical furnaces). The described parallel reduction of zinc and iron by carbon from oxides undergoes with the formation of solid metal solution of Fe–Zn containing up to 46 wt. % of zinc, melts and the vapor–gas phase of $CO–CO_2–Zn$, the equilibrium composition of which is determined by the temperature and zinc content in solid solutions and melts. The authors determined the activity and elasticity of zinc vapor in solid solutions and melts of the Fe–Zn system and the activity of components in slag melts of the $ZnO–SiO_2$ system. Thermodynamic assessment showed that in the absence of solid carbon, the reduction of zinc from oxide by carbon monoxide is possible at temperatures above 1320 °C, and reduction by iron is possible in the temperature range of 1320–1500 °C. During reduction from slag melts at reduced activity values of zinc and iron oxides and elevated temperatures, reduction of zinc is carried out more efficiently than reduction of iron. In the presence of solid carbon in all temperature ranges (above 620 °C) and concentrations of zinc and iron monoxides at values $a_{ZnO} > 0$, $a_{FeO} > 0.4$, reduction of iron undergoes more efficiently ($\Delta G^{\circ}_{FeO} < \Delta G^{\circ}_{ZnO}$). In the case of co-reduction of iron and zinc, the primary reduction product is solid iron. Thermodynamically, the possible introduction of zinc atoms into a solid solution of α-Fe is practically not realized due to the high elasticity of zinc vapor even at low concentrations in the outer layers on the surfaces of crystalline nuclei of α-Fe, which causes the possibility of a sufficiently deep degree of reduction and sublimation of zinc during its carbon-thermal reduction from concentrates and waste from metallurgical enterprises.

Keywords: zinc, metallurgical zinc – containing wastes, state diagrams of Fe – Zn, Fe – Zn – O – C, $ZnO – SiO_2$ systems, zinc activity in solid solutions and Fe – Zn melts, component activity in slag melts, zinc vapor elasticity over solid solutions and melts of Fe – Zn

For citation: Yakushevich N.F., Protopopov E.V., Temlyantsev M.V., Strokina I.V. Thermodynamic assessment of conditions for co-reduction of zinc and iron by carbon from oxides of concentrates and waste from metallurgical enterprises. *Izvestiya. Ferrous Metallurgy*. 2023;66(4):459–470. https://doi.org/10.17073/0368-0797-2023-4-459-470

Термодинамическая оценка условий совместного восстановления цинка и железа углеродом из оксидов концентратов и отходов металлургических производств

Н. Ф. Якушевич, Е. В. Протопопов, М. В. Темлянцев, И. В. Строкина

Сибирский государственный индустриальный университет (Россия, 654007, Кемеровская обл. – Кузбасс, Новокузнецк, ул. Кирова, 42)

protopopov@sibsiu.ru

Аннотация. Рассматриваются теоретические вопросы восстановления цинка и железа углеродом из оксидов концентратов и цинксодержащих металлургических отходов (пыли и шламы металлургических печей). Показана возможность параллельного восстановления цинка и железа углеродом из оксидов с образованием твердых металлических растворов Fe–Zn, содержащих до 46 % цинка (по массе), расплавов и парогазовой фазы $CO–CO_2–Zn$, равновесный состав которой определяется температурой и содержанием цинка в твердых растворах и расплавах. Определены активности и упругости пара цинка в твердых растворах и расплавах системы Fe–Zn и активности

компонентов в шлаковых расплавах системы $ZnO–SiO_2$. Термодинамическая оценка показывает, что при отсутствии твердого углерода восстановление цинка из оксида оксидом углерода CO возможно при температурах выше 1320 °C, а восстановление железом возможно в интервале температур 1320 – 1500 °C. При восстановлении из шлаковых расплавов при пониженных значениях активностей оксидов цинка и железа и повышенных температурах восстановление цинка осуществляется более эффективно, чем восстановление железа. В присутствии твердого углерода во всех диапазонах температур (выше 620 °C) и концентраций оксидов цинка ZnO и железа FeO при значениях $a_{ZnO} > 0$, $a_{FeO} > 0{,}4$ восстановление железа проходит более эффективно ($\Delta G^{\circ}_{FeO} < \Delta G^{\circ}_{ZnO}$). При совместном восстановлении железа и цинка первичным продуктом восстановления является твердое железо. Термодинамически возможное внедрение атомов цинка в твердый раствор α-железа практически не реализуется из-за высокой упругости пара цинка уже при небольших его концентрациях в наружных слоях на поверхностях кристаллических зародышей α-железа, что обуславливает возможность достаточно глубокой степени восстановления и возгонки цинка при углеродотермическом восстановлении его из концентратов и отходов металлургических производств.

Ключевые слова: цинк, металлургические цинксодержащие отходы, диаграммы состояния систем Fe–Zn, Fe–Zn–O–C, $ZnO–SiO_2$, активности цинка в твердых растворах и расплавах Fe–Zn, активности компонентов в шлаковых расплавах, упругость пара цинка над твердыми растворами и расплавами Fe–Zn

Для цитирования: Якушевич Н.Ф., Протопопов Е.В., Темлянцев М.В., Строкина И.В. Термодинамическая оценка условий совместного восстановления цинка и железа углеродом из оксидов концентратов и отходов металлургических производств. *Известия вузов. Черная металлургия*. 2023;66(4):459–470. https://doi.org/10.17073/0368-0797-2023-4-459-470

Introduction

The reduction of zinc by carbon from concentrates or metallurgical waste (dust, sludge) constitutes the primary intermediate stage in the technologies for producing zinc and zinc oxide (ZnO). Various technological options are known, implemented at temperatures ranging from 1100 to 1290 °C, including heat treatment in drum furnaces (Waelz process), multi-hearth shaft furnaces (PRIMUS process), ring furnaces (DRIVIRON process), and others. Typically, these technologies facilitate the "distillation" of zinc obtained during the vapor reduction process. Subsequently, the captured zinc vapor is condensed in apparatuses, or zinc oxide is obtained in the form of a pulverized concentrate containing up to 65 wt. % (rotary kilns) or up to 96 wt. % (multi-hearth furnaces) zinc oxide suitable for the production of electrolytic zinc metal. These zinc oxide products find application in various industries, including paint, rubber, etc. [1 – 3].

The residue remaining post zinc distillation, commonly in the form of slags containing up to 30 % iron or metallized pellets, which may contain up to 50 % (PRIMUS process) or up to 96 % (DRIVIRON process) of reduced iron metal, serves as raw material in the smelting of cast iron, steel, and ferroalloys [2].

Despite the requirement for theoretical justification for numerous technological variants, the parameters of most utilized modes are established upon the findings of kinetic studies on the reactions involving iron and zinc oxides with carbon dioxide. The practical determination of suitable parameters and designs for the involved units is crucial in this context.

A comprehensive thermodynamic analysis of the co-reduction of iron and zinc oxides is notably lacking, with insufficient consideration given to the formation of solid solutions and Fe–Zn melts, as well as chemical compounds like $ZnO·Fe_2O_3$ (zinc ferrite), $(Mn, Zn)Fe_2O_4$ (franklinite), $ZnO·Fe_2O_3$ – $2ZnO·5Fe_2O_3$ solutions. Additionally, there is an absence of information on the activities of components in Fe – Zn solid solutions, metal and slag melts, or the composition of the vapor-gas phase above these solutions and melts. The simplified schemes outlining the multiparameter mechanism of physicochemical interactions within the Fe–Zn–C–O system do not provide adequate guidance for accurately selecting the parameters of the technological regime for a specific process.

This study focuses on conducting a thermodynamic assessment of the conditions for co-reduction of zinc and iron by carbon, utilizing oxides present in metallurgical production waste such as dust and sludge. These waste materials are generated during the melting of cast iron and steel in electric arc steel-smelting furnaces and converters.

Thermodynamic analysis

Table presents the approximate composition of zinc-containing materials used in carbon-thermal reduction processes [1; 2; 4; 5].

According to [6], zincite (ZnO) and hematite (Fe_2O_3) combine to form the compound zinc ferrite ($ZnO·Fe_2O_3$), or franklinite $(Zn, Mn)Fe_2O_4$ in the presence of manganese oxide MnO. This compound remains stable in the temperature range of 700 – 1100 °C. These compounds, particularly with an excess of Fe_2O_3, create solid solutions of hematite – ferrite (or franklinite) up to the stoichiometric ratio of $2ZnO + 5Fe_2O_3$. These solutions maintain the spinel structure in its pure form up to 1100 °C. If the Fe_2O_3:ZnO ratio exceeds 2.5, sintered products contain magnetite (Fe_3O_4), is present in the sintered products; whereas a ratio lower than 1.0 results in the presence of zincite.

In dusts from arc steel smelting furnaces, characterized by 50 – 60 % Fe_2O_3, 0.5 – 4.0 % MnO and approximately 10 – 25 % ZnO [1; 2] (with a Fe_2O_3:(ZnO + MnO) ratio > 3), franklinite and magnetite are consistently present. Notably, FeO and ZnO are typically absent under these conditions.

The co-reduction of iron and zinc from dust waste follows a complex multi-stage scheme. At the first stage,

Composition of zinc-containing materials

Состав цинксодержащих материалов

Material	Content, wt. %														Reference
	Zn	Fe	SiO_2	CaO	MgO	Al_2O_3	C	Mn	Pb	Na_2O	K_2O	S	Cl	F	
Concentrate	45 – 55	5 – 15	1.0 – 5.5	0.3 – 1.2	0.2 – 0.7	1.2 – 2.7	–	–				28 – 32			[1]
EAF dust (15 – 20 kg/t steel)	18.2	30.5	4.6	7.0	2.0	1.0	2.1	2.0 – 4.0		1.5 – 2.0	2.0 – 2.5	0.45		up to 5.8	[2]
Clinker (slag of Waelz process)	1.2	30.5	28.2	7.3	2.1	1.9	1.0		3.0 – 5.0			0.4			[4]
EAF dust	12.35	44.77	3.9	7.02	9.21	0.38	10.8	2 – 4		2.94	1.0	0.4	1 – 2	0.1 – 0.4	A*
Concentrated products	45 – 55	5 – 15	1.0 – 5.5	0.3 – 1.2	0.2 – 0.7	1.2 – 2.7	–	–				28 – 32			[1]
Converter dust	5.95	34.27	3.13	15.68	7.72	1.37	10.80	0.94		1.66	2.48	0.25			A*
Zinc pitch	18 – 21	13 – 30	24 – 29	2 – 5					1.5 – 5.0				4 – 8		[2]
Converter sludge	8 – 17	3.7	5 – 10	10 – 18					0.2 – 0.3				1 – 3		[2]
Blast furnace sludge from West Siberian Metallurgical Combine	6 – 10	28 – 35	4 – 8	3.0 – 5.9	1.7 – 2.0	1.6 – 4.0	18 – 34			1.0 – 1.6	0.10 – 0.15	2.4 – 3.3			[5]
Pyrolysis product of rubber tires	8.24	5.55	12.38	1.93	0.48	1.69	56.81	0.12		1.63	0.44	4.20			A*

Note. A* based on the analysis results of samples from EVRAZ JSC.

within a reducing atmosphere, zinc ferrite readily undergoes decomposition through the reaction

$$ZnO{\cdot}Fe_2O_3 + 1/3CO = ZnO + 2/3Fe_3O_4 + 1/3CO_2. \quad (1)$$

At the second stage, higher iron oxides present in zinc-containing materials, along with the magnetite formed during the ferrite decomposition, are reduced by gaseous carbon monoxide CO in accordance with the reactions:

$$3Fe_2O_3 + CO = 2Fe_3O_4 + CO_2; \quad (2)$$

$$Fe_3O_4 + CO = 3FeO + CO_2. \quad (3)$$

Reaction (3) is achieved at 550 °C when the carbon monoxide content (in the gas phase composed of CO and CO_2) is approximately 50 %. At 640 °C, the equilibrium P_{CO} is roughly 0.4. At higher temperatures, reaction (3) can occur at low concentrations of carbon monoxide (CO): at 1000 °C $P_{CO} \approx 0{,}2$ atm; at 1200 °C $P_{CO} \approx 0.1$ atm [7].

At the third stage, reduction of iron from wustite with carbon monoxide CO occurs through the reaction

$$FeO(s) + CO = Fe(s) + CO_2 \quad (4)$$

this reduction process takes place at elevated concentrations of carbon monoxide CO in the gas phase. Specifically, at 700 °C $P_{CO} \geq 0.6$ atm, $CO{:}CO_2 \approx 1.5$; at 400 °C $P_{CO} \geq 0.68$ atm, $CO{:}CO_2 \approx 2$; at 1300 °C $P_{CO} \geq 0.76$ atm, $CO{:}CO_2 \approx 2.7$ [8]).

The reduction of zinc from oxide occurs through the reaction

$$ZnO(s) + CO = Zn(l, g) + CO_2, \quad (5)$$

however, this process is intricate due to intense zinc evaporation and the formation of α-Fe–Zn solid solutions and Fe–Zn melts.

In the presence of solid carbon or the potential for its formation during the decomposition of carbon monoxide (CO), the reduction of oxides at all stages can be achieved through direct contact interaction with solid carbon, known as direct reduction. Thermodynamically, this process is more favorable; however, its efficient implementation requires fine grinding and thorough mixing of the reagents to maximize the interaction surface. The composition of the equilibrium gas phase in this case is constrained by the equilibrium of the Boudoir reaction

$$CO_2 + C = 2CO. \quad (6)$$

For the practical implementation of carbon-thermal reduction technologies, it is crucial to determine the parameters of phase-chemical interactions occurring at the third and final stage of the process.

The thermodynamic analysis was based on the following initial data: one of the latest versions of the state diagram of the iron–zinc system [9], which notably differs from those previously presented in reference literature (refer to Fig. 1 in [10]); the phase chemical equilibrium diagram of the Fe–C–O system (see Fig. 4 in [11]); and reference data concerning the thermodynamic properties of iron, zinc, and carbon oxides [12 – 14].

According to the state diagram of Fe–Zn alloys [9], zinc undergoes melting at a temperature of 419.6 °C (forming a eutectic with less than 0.1 % Fe at 419.4 °C). As the temperature increases to 531 °C, the solubility of iron in the zinc melt rises, reaching approximately 2.5 %. Upon exceeding the equilibrium iron concentrations, a solid solution, known as the ζ phase (Zn ≈ 94 ÷ 97 %), precipitates from the melt. At 531 °C, the ζ phase undergoes decomposition through a peritectic reaction, giving rise to the δ_1 phase (solid solution Zn ≈ 88 ÷ 92 %). The δ_1 phase coexists with the "Γ_1" phase (81 – 86 % Zn), until 550 °C, at which point it decomposes, forming the "Γ" phase. The "Γ" phase coexists with the δ and α-iron phases up to 667 – 780 °C. In the temperature range of 667 – 780 °C, it coexists with α-ferrite and a liquid melt containing iron ranging from 2.5 to 8.5 %. At 780 °C, the "Γ" phase undergoes decomposi-

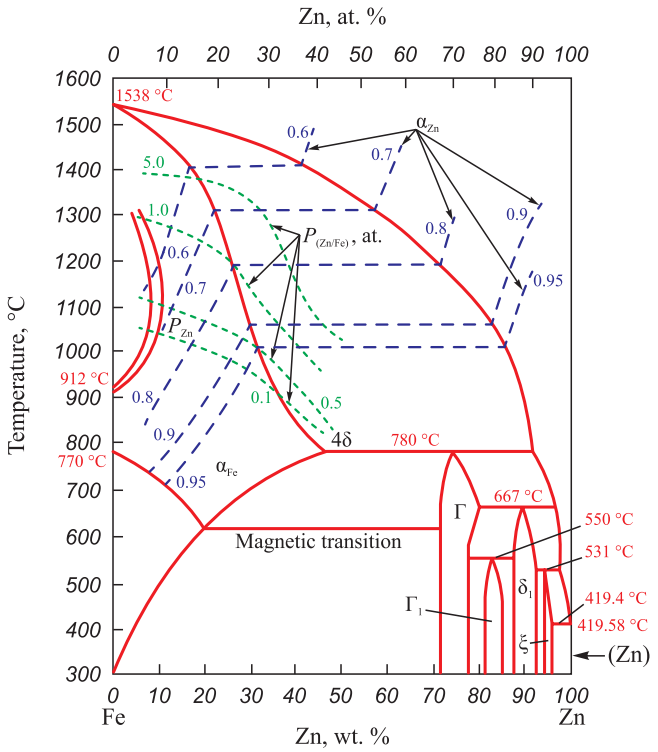

Fig. 1. State diagram of the Fe–Zn system:
– – – zinc activity in solid solutions and Fe–Zn melts;
——— P_{Zn} – elasticity of zinc vapor over Fe–Zn solid solutions;
– – – α_{Zn} – Fe – Zn solid solutions

Рис. 1. Диаграмма состояния системы Fe–Zn:
– – – активности цинка в твердых растворах и расплавах Fe–Zn;
——— P_{Zn} – упругость пара цинка над твердыми растворами Fe–Zn;
– – – α_{Zn} – твердые растворы Fe–Zn

tion through a peritectic reaction into a liquid melt containing approximately 8 % iron and a solid solution based on α ferrite with a zinc content of 46 %. At temperatures lower (300 °C) and higher (up to 1535 °C), the zinc content in the ferrite solution decreases nearly to zero. Consequently, the region of Fe – Zn solid solutions extends within the range of zinc concentrations of 0 – 46 % in the solution and temperatures of 0 – 1535 °C. Additionally, there exists a broader two-phase region, encompassing iron-based solid solutions containing 0 – 46 % Zn and liquid Fe – Zn melts with a zinc content ranging from 0 (at 153 °C) to 92 % (at 780 °C).

Fe – Zn solid solutions based on α ferrite undergo a magnetic transformation within the temperature range of 769 °C (0 % Zn) to 623 °C (20 % Zn).

Zinc exhibits high vapor elasticity, and its vapor pressure above pure zinc follows the equation

$$\lg P^{\circ}_{Zn} = -\frac{6171}{T} + 5.423,$$

according to this equation $P^{\circ}_{Zn} = 0.1$ atm at 720 °C, $P^{\circ}_{Zn} = 1$ atm at 907 °C, $P^{\circ}_{Zn} = 10$ atm at 1183 °C, $P^{\circ}_{Zn} = 57$ atm at 1500 °C. Equilibrium zinc vapor pressures above solid solutions of α-Fe – Zn and melts vary in accordance with changes in the activity of zinc in them and temperature, described by the equation $a_{ZnO} = f(x_{Zn}, T)$.

Due to the lack of data on the activities of components in the Fe – Zn system, the Fe – Cu system was employed as a prototype. In the Fe – Cu system, a broad range of solid solutions based on α-Fe – Cu ferrite (Cu ≈ 0 ÷ 8 %) exists, bordering in the temperature range of 1094 – 1484 °C with an even wider two-phase region: solid solution (α-Fe) – melt (Cu = $8_{(1484\,°C)} \div 97_{(1094\,°)}$ %) [10]. Substantial positive deviations from Raoult's law are observed in Fe – Cu melts. At 1550 °C in Fe – Cu melts with a copper content of 0 – 4 % $\gamma_{Cu} = 10.1$. With an increase in the concentration of copper in the melt, the activity of copper decreases: at $x_{Cu} = 0.1$ (10 %) – $\gamma_{Cu} = 5.4$, $a_{Cu} = 0.56$; at $x_{Cu} = 0.2$ (18 %) – $\gamma_{Cu} = 13.8$, $a_{Cu} = 0.71$; at $x_{Cu} = 0.4$ (37 %) – $\gamma_{Cu} = 2.0$, $a_{Cu} = 0.8$; at $x_{Cu} = 0.8$ (70 %) – $\gamma_{Cu} = 1.2$, $a_{Cu} = 0.89$ [15]. It is noteworthy that in homogeneous melts with positive deviations from Raoult's law, these positive deviations increase as the temperature decreases. When the concentration dependence lines reach $a_i = f(x_i, T) = \text{const}$ for compositions corresponding to x_i of the liquidus at a given temperature, the values of a_i within the two-phase region remain constant until the x_i of the solidus is reached. Simultaneously, positive deviations from Raoult's law increase even more. Furthermore, the activity of components in a homogeneous solid solution decreases as their concentration in the solution decreases.

The values of activities and activity coefficients of zinc in Fe – Zn solid solutions and melts, as per these assumptions, are depicted in Fig. 2.

In melts with high zinc content (more than 50 %), zinc activity coefficients exhibit minimal deviation from unity, and zinc activities demonstrate slight positive deviations from Raoult's law. In solid solutions with a zinc content ranging from 5 to 25 % and temperatures between 1000 and 1400 °C, the activity of zinc varies from 0.5 to 0.9, and the activity coefficients are $\gamma_{Zn} = 5 \div 9$, indicating substantial positive deviations from Raoult's law.

Consequently, even above solid solutions (α-Fe, Zn) containing relatively small amounts of zinc (5 – 10 %), the vapor pressure of zinc is substantial. The equilibrium values of zinc activities in solid solutions and melts, along with the vapor pressure of zinc above solid solutions, are plotted on the state diagram of the Fe – Zn system (Fig. 1). Based on the provided data, it can be inferred that at a zinc content in the α-iron solid solution of 5 – 10 %, the vapor pressure of zinc at $t \approx 1050$ °C reaches 0.5 atm, and at 1300 °C, it surpasses 1 atm. As the zinc concentration in the solid solution increases, the vapor pressure of zinc also increases. For instance, $t \approx 1050$ °C, it attains 0.1 atm and 0.5 atm at 5 and 20 % zinc content, respectively.

The outcomes of thermodynamic analysis of the reduction of iron and zinc from oxides are depicted in Fig. 3 as dependences of the functions $\Delta G° = f(T)$, reduced to 1 mole of oxygen in the initial gas phase for oxide formation reactions, and the corresponding number of moles of the initial oxide for reduction reactions.

The reduction of iron from wustite by carbon monoxide CO through reaction (4)

$$2FeO(s, l) + 2CO = 2Fe(s) + 2CO_2$$

initiates at 580 °C in the absence of solid carbon (point *F* in Fig. 3, where the lines $\Delta G° = f(T)$ for reactions (6) and (7) intersect):

$$2CO + O_2 = 2CO_2;$$

$$2Fe(s) + O_2 = 2FeO(s). \qquad (7)$$

For reaction (4) at $t = 580$ °C $\Delta G^{\circ}_{(4)} = 0$ ((point *F*′), $P_{CO}:P_{CO_2} = 1$, $P_{O_2} \approx 10^{-25}$ atm; at $t = 1200$ °C $\Delta G^{\circ}_{(4)} = -25$ kJ; at $t = 1500$ °C $\Delta G^{\circ}_{(4)} = -55$ kJ.

The reduction of zinc from zincite by carbon monoxide CO through reaction (5)

$$2ZnO(s) + 2CO = 2Zn(g) + 2CO_2$$

commences at higher temperatures. For the point *L*′ in Fig. 3 $t_{start} \approx 1320$ °C, $\Delta G^{\circ}_{(5)} = 0$, $P_{O_2} \approx 10^{-10}$ atm; at $t = 1500$ °C $\Delta G^{\circ}_{(5)} = -55$ kJ. At $t = 1500$ °C the lines $\Delta G° = f(T)$ for reactions (4) and (5) at intersect at $\Delta G^{\circ}_{(4)} = \Delta G^{\circ}_{(5)} = -55$ kJ (point *D* in Fig. 3).

At temperatures lower than 1500 °C $\Delta G^{\circ}_{(4)} < \Delta G^{\circ}_{(5)}$, at $t > 1500$ °C $\Delta G^{\circ}_{(5)} < \Delta G^{\circ}_{(4)}$. It can be assumed that in

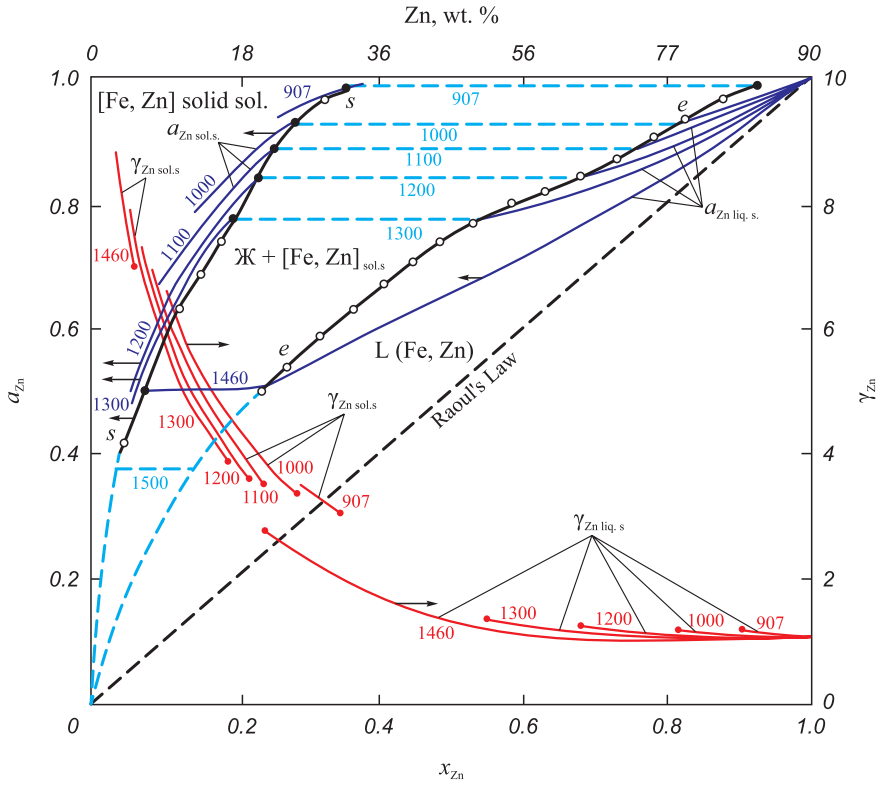

Fig. 2. Dependence of zinc activity and activity coefficient on composition and temperature

Рис. 2. Зависимость активности и коэффициента активности цинка от состава и температуры

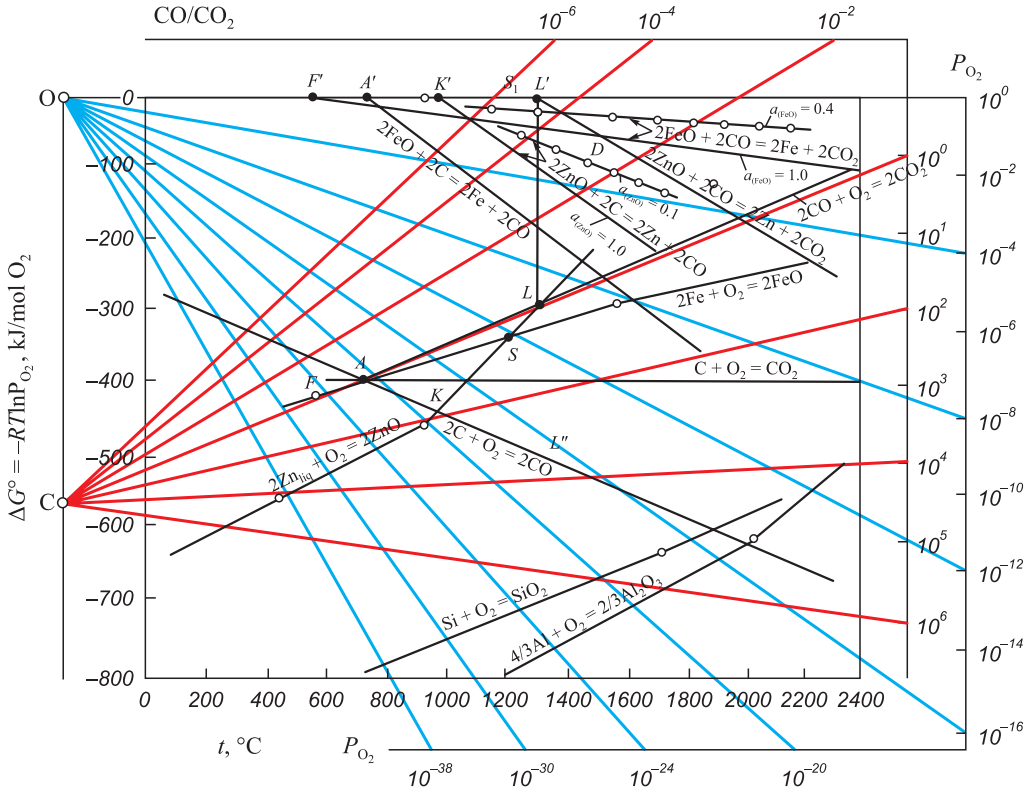

Fig. 3. Dependence of Gibbs energy and equilibrium compositions of the gas phase ($CO:CO_2$; P_{O_2}) on temperature for reactions of oxides formation and for reactions of reduction of iron and zinc by carbon and CO oxide

Рис. 3. Зависимость энергии Гиббса и равновесных составов газовой фазы ($CO:CO_2$; P_{O_2}) от температуры для реакций образования оксидов и для реакций восстановления железа и цинка углеродом и оксидом CO

the temperature range of 1320 – 1500 °C, under the conditions of a reducing atmosphere required for the production of iron metal by reaction (1) – (P_{CO}:P_{CO_2} > 1, P_{O_2} < 10^{-8} atm), reduced iron can act as a zinc-reducing agent from zincite. At higher temperatures, zinc vapor can reduce iron from wustite:

$$Fe(s, l) + ZnO(s) \underset{>1500\ °C}{\overset{1320\div1500\ °C}{\rightleftarrows}} Zn(g) + FeO(s, l). \quad (8)$$

Thus, the reduction of zinc from zincite by carbon monoxide CO is possible only at temperatures above 1320 °C (400 °C above the boiling point of zinc), with zinc obtained only in the vapor state. In practice, reactions (4), (5), and (8) proceed in parallel, and the reduced iron acts as a catalyst for reaction (5). The practical realization of the indirect reduction process is not realistic due to the low values of $\Delta G°$ for reactions (4), (5), (8).

The processes of iron and zinc reduction from oxides by solid carbon are governed by reactions (9) and (10):

$$2FeO(s, l) + 2C(s) = 2Fe(s, l) + 2CO; \quad (9)$$

$$2ZnO(s) + 2C(s) = 2Zn(l, g) + 2CO. \quad (10)$$

The initiation of reduction for reaction (9) is characterized in Fig. 3 by point *A*: the intersection of lines $\Delta G° = f(T)$ for reactions (6) and (11):

$$2C + O_2 = 2CO, \quad (11)$$

for reaction (10), it is marked by point *K*: the intersection of lines $\Delta G° = f(T)$ for reactions (11) and (12):

$$2Zn(g) + O_2 = 2ZnO(s). \quad (12)$$

Parameters of point *A*: $t_{start} \approx 650$ °C, P_{CO}:$P_{CO_2} \approx 1.1$, $P_{O_2} \approx 10^{-21}$ atm; $\Delta G^{\circ}_{(9)start} = 0$ (point *A′*); for point *K*: $t_{start} \approx 960$ °C (approximately 330 °C lower than for reaction (5)), P_{CO}:$P_{CO_2} \approx 10^2$, $P_{O_2} \approx 10^{-19}$atm; $\Delta G^{\circ}_{(10)start} = 0$ (point *K′*).

Above 960 °C, in the entire temperature range, reaction (9) has a significant advantage over reaction (10) ($\Delta G^{\circ}_{(9)} - \Delta G^{\circ}_{(10)} = -80$ kJ).

During the co-reduction of iron and zinc, the presence of carbon facilitates the formation of the ternary carbide Fe_3ZnC [12]. This carbide coexists at temperatures of at least 780 °C with α-iron (with a zinc content in a solid solution based on α-iron lower than 46 % and carbon higher than 4 %) and the "Γ" phase with a zinc content of 71 – 74 %. The "Γ" phase decomposes at 780 °C through a peritectic reaction (13) with the formation of α-iron and a liquid phase containing approximately 7 % Fe, 89 % Zn, 4 % C:

$$\text{"}\Gamma\text{"} \rightarrow (\alpha\text{-Fe} + Zn) + l. \quad (13)$$

The presence of carbon restricts the reduction processes by limiting the composition of the gas phase ($CO:CO_2$ ratio) in accordance with the equilibrium constant of the Boudoir reaction (6).

The presented volumetric diagram (Fig. 4, face *A*) indicates that in the presence of solid carbon, the reduction temperature of iron from wustite corresponds to $t_{start} \approx 690$ °C (for the formation of cementite Fe_3C $t_{start} \approx 680$ °C) with the $CO:CO_2$ ratio in the gas phase approximately 1.5. In the presence of excess carbon, the concentration of carbon monoxide CO in the gas phase aligns with the equilibrium for reaction (6). The $CO:CO_2$ ratio at 690 °C is approximately 1.5; at 900 °C, it is approximately 19; at higher temperatures, the content of carbon monoxide CO is almost 100 % ($CO:CO_2 \geq 10^2$) (Fig. 4).

Similarly, during the reduction of zinc by carbon according to reaction (10) at the start temperature of the reduction $t_{start} \approx 960$ °C and higher $CO:CO_2 \geq 10^2$.

It is worth noting that at low temperatures (below 1200 °C), the activities of iron and carbon show slight deviations from their molar concentrations [14], and their variations in Fe – Zn solid solutions and melts do not significantly affect the equilibrium of reactions (9) and (10).

During the carbothermal co-reduction of a mixture of zinc and iron oxides, the primary reduction product consists of crystalline iron nuclei formed by reactions (1) (in the temperature range 580 – 1535 °C) and (5) (above 700 °C until the formation of the iron-carbon melt). The reduction of zinc with its transition into iron nuclei, along with the formation of solid solutions based on α-iron, begins almost simultaneously with the emergence of a new phase (α-iron). This process is similar to what occurs during the co-reduction of manganese and silicon, where primary small drops of metal (MnC_x) with 5 – 8 % silicon are present [16]. In the melting of calcium carbide, in the primary drops of metal formed in the low-temperature levels of the ore smelting furnace bath, up to 8 % silicon in the ferrous alloy is also detected. It is noteworthy that in Mn – Si and Fe – Si alloys, there are strong negative deviations from Raoult's law ($\gamma_{Si} \approx 10^{-3}$), and in Fe – Zn alloys with low zinc concentrations ($x_{Zn} < 0.2$), there are positive deviations $\gamma_{Zn[Fe]} = 4 \div 10$ (Fig. 2). Considering the high vapor elasticity of zinc and the potential formation of low-melting films of melts on the surface of α-iron nuclei, along with the intense evaporation of zinc from their surfaces, and the kinetic challenges associated with zinc diffusion inside solid-phase nuclei, it can be assumed that most of the zinc transitions into the vapor-gas phase. Consequently, the equilibrium states of solid metal – slag – gas are practically unattainable due to these factors.

The calculated thermodynamic parameters of the Fe – – Zn – O – C system are illustrated in Fig. 4. The analysis reveals that achieving a concentration of 5 ÷ 10 % Zn in the α-Fe solid solution is possible at temperatures

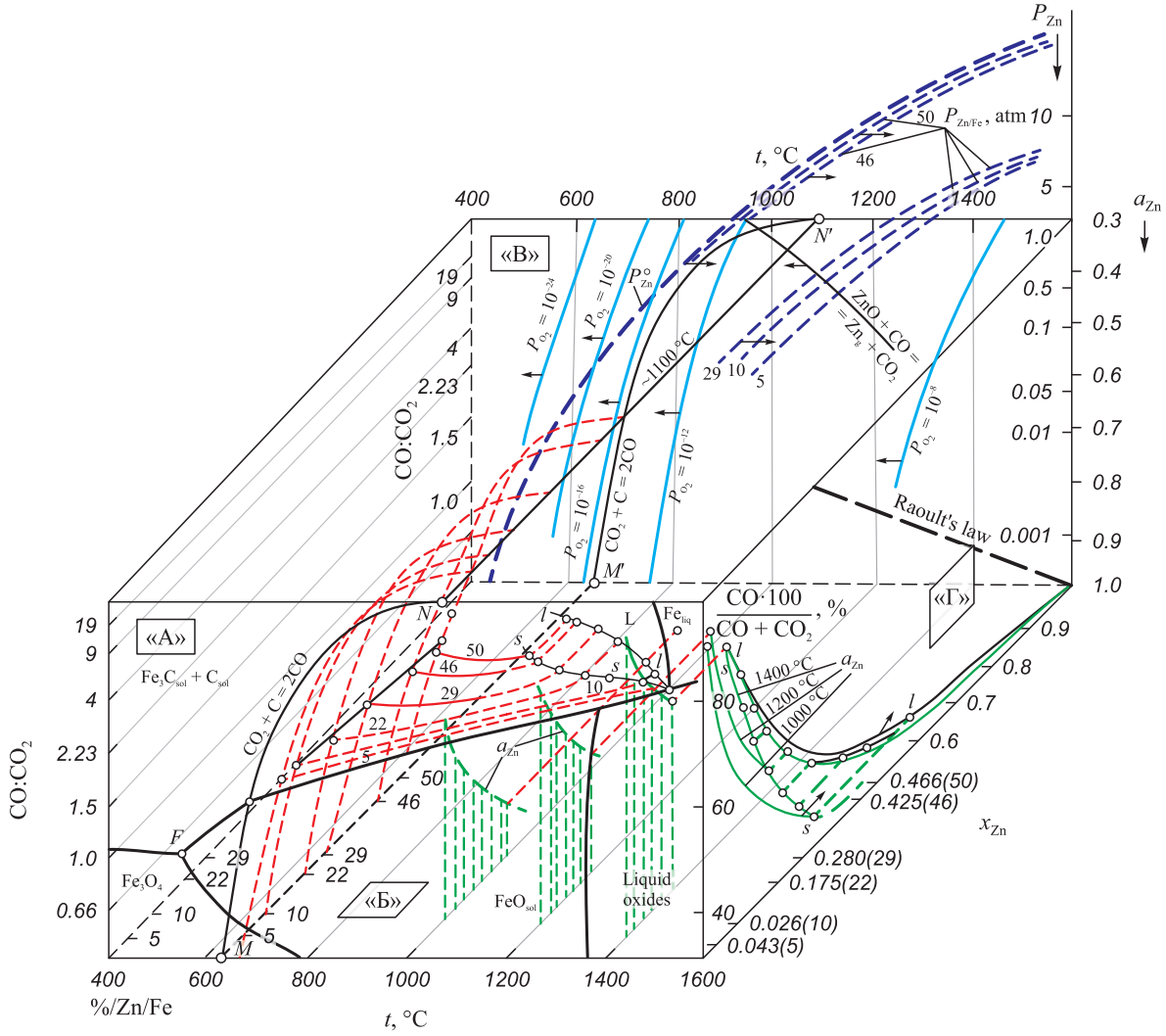

Fig. 4. Physico-chemical parameters of the Fe–Zn–O–C system (–o– – lines of liquidus (l – l) and solidus (s – s)

Рис. 4. Физико-химические параметры системы Fe–Zn–O–C (–o– – линии ликвидуса (l – l) и солидуса (s – s)

between 700 – 800 °C, with $a_{Zn} = 0.9$, and an equilibrium vapor pressure of zinc at approximately 0.01 atm (Fig. 1). In surface films that are supersaturated with zinc $P_{Zn} > 0.1$ atm, reaching 1 atm at 1300 – 1200 °C.

Results and discussion

The feasibility of co-reducing iron and zinc, leading to the formation of Fe–Zn solid solutions, is highly contingent on various factors such as temperature, heating rate, isothermal holding time, solubility, and the energy of formation of solutions.

For instance, when carbon interacts with silica particles smaller than 100 μm, the reduction rate increases by 2 – 3 orders of magnitude [17].

It can be postulated that factors such as the degree of grinding, mixing, and compacting of reagents, involving briquetting and agglomeration, could lead to a substantial increase in the reaction surface area. This increase, accompanied by elevated excess energy due to mechano-energetic activation during mechanical processes, might result in a lower initiation temperature for the co-reduction of iron and zinc, a rapid acceleration of reactions, and the potential formation of Fe–Zn solid solutions with a notably high concentration of zinc.

The optimal mixing of iron and zinc oxides is achieved when the components are combined at the molecular level in chemical compounds such as ferrite and franklinite, or at high temperatures in slag melts. Research [1] has demonstrated that zinc recovery from ferrite occurs more rapidly and at lower temperatures (~800 °C) compared to pure zincite (~1000 °C). Even at temperatures between 800 – 900 °C, zinc is significantly reduced (at 800 °C $P^{\circ}_{Zn} \approx 0.6$ atm; at 900 °C $P^{\circ}_{Zn} > 0.9$ atm).

The reduction of iron and zinc from slag melts by carbon monoxide CO is influenced by temperature, the composition of the gas phase, the melt composition, and, consequently, the activity of FeO oxide in the melt. Additionally, it depends on the physical characteristics of the melt, including homogeneity, viscosity, interfa-

cial surface tension between slag-metal and slag – gas, the degree of surface interaction influenced by the amount of slag and gas, as well as the degree of bubbling and emulsification of heterogeneous slag.

When reducing iron and zinc from slag with solid carbon, properties of the carbon reducing agent, including reactivity, porosity, density, fractional composition, and wettability with metal and slag melts, become significant factors.

In the $FeO - SiO_2$ system slags saturated with silica, the activity of iron oxide FeO when its content in the melt is 0 – 55 % ($x_{FeO} < 0.5$) exhibits little dependence on the composition and temperature (at 1350 – 1600 °C $a_{FeO} = 0.36 \div 0.37$ [10; 18]. In the presence of basic oxides, for example, like slags of the $FeO - SiO_2 - (CaO + MgO)$ system, positive deviations from Raoult's law are observed at 1600 °C in the FeO concentration range of 0 – 50 %, with the magnitude increasing with higher slag basicity $R = CaO:SiO_2$ and lower temperature. For instance, at 1600 °C in slags saturated with silica ($SiO_2 = 50 \div 60$ %), and iron oxide FeO content of 10, 20, 30 and 40 %, the activities a_{FeO} are 0.15, 0.29, 0.45, and 0.55, respectively. Increasing slag basicity R to 1 results in approximately a 1.5 times increase in the activity of iron oxide. Similar findings were obtained in [1; 19] at 1250 and 1200 °C for slags containing 25 – 60 % FeO with basicity ranging from 0.33 – 1.0.

Therefore, from slags with $R < 1$ at $a_{FeO} < 1$ the reduction of iron by carbon monoxide CO is more challenging compared to pure oxide.

A similar conclusion can be drawn regarding reaction (5). The shift of lines of equilibrium $\Delta G^\circ = f(T)$ for reaction (4) at $a_{FeO} = 0.4$ is shown in Fig. 3.

In most carbothermal technological processes designed for zinc recovery from concentrates and industrial waste (e.g., Waelz process, PRIMUS, etc.), measures are taken to prevent the formation of large amounts of low-melting liquid metal and complex oxide eutectic melts at process temperatures ranging from 1150 – 1250 °C. This is achieved by incorporating sand and an excess (up to four times the stoichiometric requirement) of a larger (up to 5 mm) carbonaceous reducing agent into the charge mixture as thickeners. The addition of these thickeners results in the formation of a viscous heterogeneous slag with a high content of silicon oxide (up to 30 – 40 %), leading to a significant decrease in the activity of the main oxides, including ZnO, in the slag. This complicates the recovery of zinc.

The interaction between zinc and silicon oxides gives rise to a double chemical compound, $2ZnO \cdot SiO_2$ commonly known as willemite, with a ZnO content of 73 %. Willemite undergoes congruent melting at 1512 °C and forms eutectics with ZnO (SiO_2 – 21 %, t = 1505 °C) and with SiO_2 (SiO_2 – 43 %, t = 1430 °C) (Fig. 5, *a*). At temperatures below 1430 °C within the ZnO concentrations in the range of 0 – 73 %, only solid phases coexist in the $ZnO - SiO_2$ system: SiO_2 and $2ZnO \cdot SiO_2$.

In the presence or addition of basic oxides (CaO, MgO, FeO, MnO) to the charge mixture, the melting temperature of the slag decreases (in the $e_1 - E_t$ direction, as shown in Fig. 5, *a*) reaching the temperatures of ternary or more complex eutectics (around ~1000 °C), and even lower in the presence of Na_2O (down to 800 °C). This can lead to the formation of complex zinc-containing compounds, such as $xMeO \cdot yZnO \cdot zSiO_2$ (x, y, z = 1 or 2).

The activity of zinc oxide a_{Zn} in eutectic melts can vary significantly and reach 0.1, significantly complicating the reduction of zinc. Fig. 3 illustrates the change in the parameters of the function $\Delta G^\circ = f(T)$ for reaction (10) at $a_{Zn} = 1$ and $a_{Zn} = 0.1$. At 1200 °C, the difference between $\Delta G_{(10)}$ at $a_{Zn} = 1$ and $a_{Zn} = 0.1$ is ~30 % (70 and 50 kJ). It has been observed that in slags with a zinc content of 0.5 – 10 %, the replacement of calcium oxide with iron oxide FeO does not alter the activity coefficient of zinc oxide. However, a change in the content of the mole fraction of silicon oxide from 0.26 – 0.30 to 0.35 – 0.40 reduces the activity coefficient of zinc oxide by 2.1 – 2.5 times. Further increases in the SiO_2 content in the slag to 44 – 46 mol. % (slags saturated with silica) does not affect the value of the activity coefficient of zinc oxide.

Changes in the activities of components in the $ZnO - SiO_2$ system at 1500 and 1600 °C are shown in Fig. 5, *b* (the diagram shows isoactivity lines $a_{ZnO} = f(x_{SiO_2}, t = \text{const})$ and $a_{ZnO} = f(x_{SiO_2}, t = \text{const})$ (Fig. 5, *a*). The presence of two phase regions in the state diagram of the $ZnO - SiO_2$ system determined the sign alternating dependence of the activity isotherms of the components and their intersection with the lines of Raoult's law at points $R_i (a_i = x_i, \gamma_i = 1)$, which makes it possible to fairly correctly represent the course of activity isotherms [10].

It was demonstrated in [20] that in three-component (and more complex) systems, even in acidic slags (at the line of saturation with silica) with the addition of basic oxides (CaO, MgO, etc.), their activity in primary slags formed at the beginning of melting change by orders of magnitude (from 0.1 – 0.6 to ~0.001). Accurate information for a specific technological option and a given mode (charge composition, temperature) can be obtained through experimental studies.

Conclusions

Utilizing existing reference data and kinetic studies, a thermodynamic assessment of the co-reduction conditions of zinc and iron by carbon from oxides present in concentrates and by-products of metallurgical processes (such as dust and sludge generated during steel melting in electric arc furnaces and converters) was conducted.

Graphs depicting the zinc activity in solid metal solutions based on α-iron and Fe – Zn melts were created, illustrating their composition and temperature dependence.

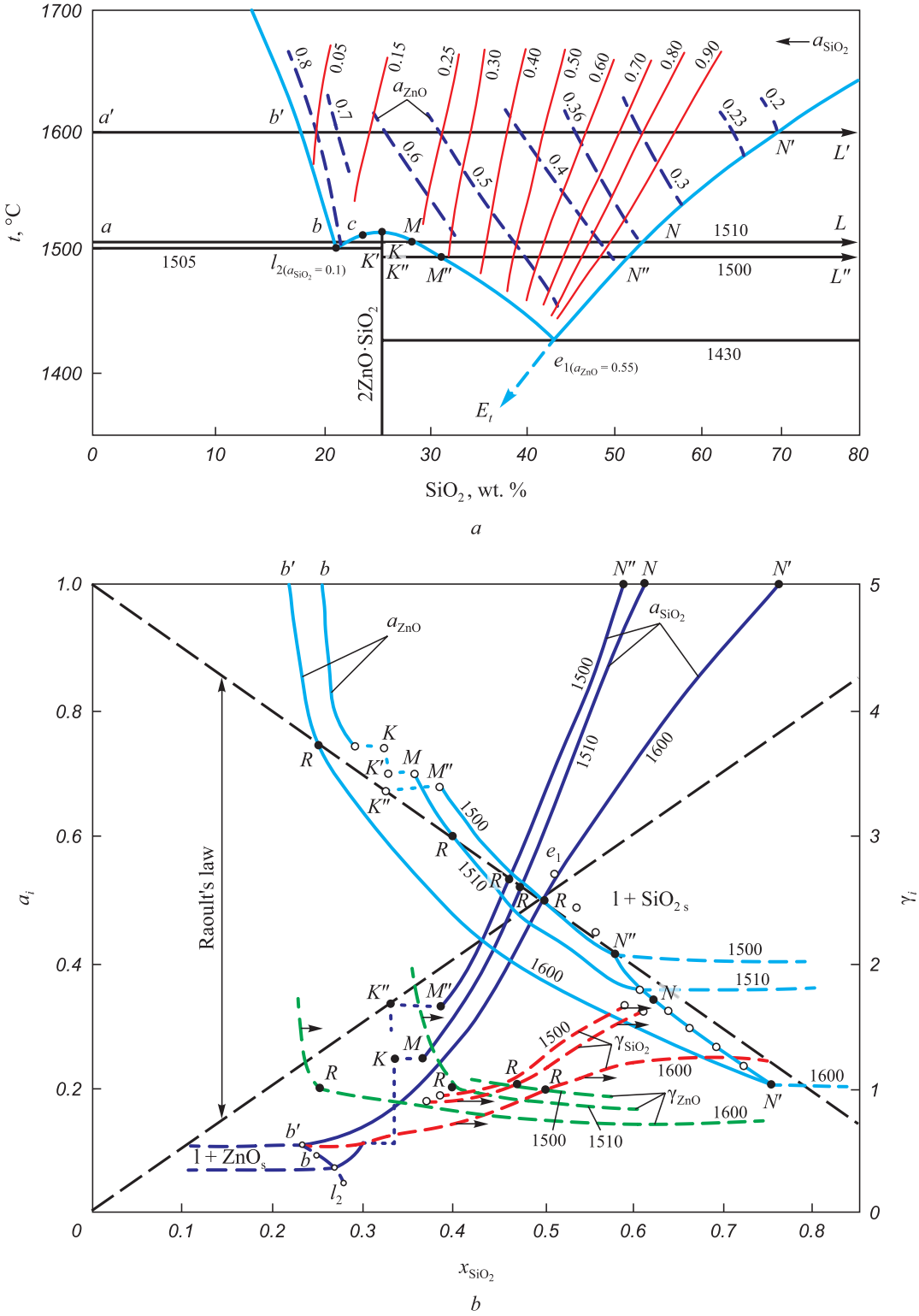

Fig. 5. Diagram of the state of the ZnO–SiO_2 system (*a*) and the activity and activity coefficients of the components in the ZnO–SiO_2 system (*b*): –○– $N'–N–N''–l_1$ and $в'–в–l_2$ – boundaries of the two-phase zones l + ZnO(s)

Рис. 5. Диаграмма состояния системы ZnO–SiO_2 (*a*) и активности и коэффициенты активности компонентов в системе ZnO–SiO_2 (*b*): –○– $N'–N–N''–l_1$ и $в'–в–l_2$ – границы двухфазных областей l + ZnO(s)

The activities of a_{ZnO} and a_{SiO_2} in ZnO–SiO_2 homogeneous melts at 1500 and 1600 °C were also charted. It is evident that in silica-saturated slags, the activity of zinc oxides decreases from 0.37 at 1430 °C to 0.2 at 1600 °C.

The absence of solid carbon in the system allows zinc recovery from oxide by carbon monoxide CO at temperatures above 1320 °C. However, with the presence of solid carbon, zinc reduction can occur at lower temperatures

(300 – 350 °C). At 1200 °C and $a_{ZnO} = 1$ $\Delta G_{(10)} \approx 50$ kJ, at ~1350 °C $\Delta G_{(10)} = 100$ kJ. The reduction from slags at $a_{ZnO} \leq 0.1$ requires higher temperatures (by 150 – 300 °C, respectively).

During co-reduction of zinc and iron from oxides with solid carbon, the primary reduction product is solid α-iron. At temperatures above 1000 °C, reduced iron acts as a reducing agent and catalyst for the zinc reduction reaction.

Zinc exhibits intensive evaporation from Fe – Zn metal melts and α-Fe – Zn solid solutions, including solid crystalline nuclei. Even with a zinc content in solutions of less than 5 % at 1300 °C, the equilibrium pressure of zinc vapor above the solutions reaches 1 atm, facilitating a high degree of dezincification of zinc-containing concentrates and metallurgical waste through carbothermal reduction methods.

References / Список литературы

1. Lakernik M.M. *Electrothermy in Metallurgy of Copper, Lead, Zinc*. Moscow: Metallurgiya; 1971:296. (In Russ.).

   Лакерник М.М. *Электротермия в металлургии меди, свинца, цинка*. Москва: Металлургия; 1971:296.
2. Tarasov A.V., Besser A.D., Mal'tsev V.I. *Metallurgical Processing of Secondary Zinc Raw Materials*. Moscow: Gintsvetmet; 2004:219. (In Russ.).

   Тарасов А.В., Бессер А.Д., Мальцев В.И. *Металлургическая переработка вторичного цинкового сырья*. Москва: Гинцветмет; 2004:219.
3. Saramak D., Krawczykowski D., Gawenda T. Investigations of zinc recovery from metallurgical waste. *IOP Conference Series: Materials Science and Engineering*. 2018;427:012017. https://doi.org/10.1088/1757-899X/427/1/012017
4. Kozlov P.A. *Veltz-Process*. Moscow: Ruda i metally; 2002:175. (In Russ.).

   Козлов П.А. *Вельц-процесс*. Москва: ИД «Руда и металлы», 2002:175.
5. Kuznetsov S.N., Volynkina E.P., Protopopov E.V., Zorya I.V. *Metallurgical Technologies for Processing Technogenic Deposits, Industrial and Household Waste*. Novosibirsk: Publishing House of the SB RAS; 2014:294. (In Russ.).

   Металлургические технологии переработки техногенных месторождений, промышленных и бытовых отходов / С.Н. Кузнецов, Е.П. Волынкина, Е.В. Протопопов, И.В. Зоря. Новосибирск: Изд-во СО РАН; 2014:294.
6. Ivanovskaya M.I., Tolstik A.I., Kotikov D.A., Pan'kov V.V. Structural features of Zn – Mn-ferrite synthesized by pyrilysis sputtering. *Zhurnal fizicheskoi khimii*. 2009;83(12): 2283–2288. (In Russ.).

   Ивановская М.И., Толстик А.И., Котиков Д.А., Панькова В.В. Структурные особенности Zn – Mn-феррита, синтезированного методом распылительного пиролиза. *Журнал физической химии*. 2009;83(12):2283–2288.
7. Dinel't V.M., Anikin A.E., Strakhov V.M. Reduction of iron ore by means of lignite semicoke. *Coke and chemistry*. 2011;54(5):165–168. https://doi.org/10.3103/S1068364X11050048
8. Nokhrina O.I., Rozhihina I.D., Hodosov I.E. The use of coal in a solid phase reduction of iron oxide. *IOP Conference Series: Materials Science and Engineering*. 2015;91:012045. https://doi.org/10.1088/1757-899X/91/1/012045
9. *State Diagrams of Double Metal Systems. Guide*. Lyakishev N.P. ed. Moscow: Mashinostroenie; 1997:1024. (In Russ.).

   Диаграммы состояния двойных металлических систем. Справочник / Под общ. ред. Н.П. Лякишева. Москва: Машиностроение; 1997:1024.
10. Elliott John F., Gleiser Molly, Ramakrishna V. *Thermochemistry for Steelmaking*. Addison – Wesley Inc.; 1963.

    Эллиот Д.Ф., Глейзер М., Рамакршина В. *Термохимия сталеплавильных процессов*. Москва: Металлургия; 1969:252.
11. Shcherban A.P. Dependence of interphase distribution coefficients on temperature and concentration of components in double metal systems. *East European Journal of Physics*. 2020;(4):63–68. https://doi.org/10.26565/2312-4334-2020-4-08
12. Kubaschewski O. *Iron – Binary Phase Diagrams*. Berlin; 1982.

    Кубашевски О. *Диаграммы состояния двойных и многокомпонентных систем на основе железа*. Москва: Металлургия, 1985:184.
13. Khina B.B., Goranskiy G.G. Thermodynamic properties of multicomponent amorphous alloys in Fe–Si–B–Ni and Fe–Si–B–Ni–CO–Cr–Mo systems. *Advanced Materials and Technologies*. 2016;(2):8–15. https://doi.org/10.17277/amt.2016.02.pp.008-015
14. Massardier V., Merlin J., Le Patezour E., Soler M. Mn–C interaction in Fe–C–Mn steels: Study by thermoelectric power and internal friction. *Metallurgical and Materials Transactions A*. 2005;36:1745–1755. https://doi.org/10.1007/s11661-005-0039-x
15. Yakushevich N. F., Kaveshnikov A.A. Thermodynamic analysis of the CaO – SiO_2 – TiO_2 system as part of invariant equilibria. *Izvestiya. Ferrous Metallurgy*. 2004;47(6):7–11. (In Russ.).

    Якушевич Н. Ф., Кавешников А.А. Термодинамический анализ системы CaO – SiO_2 – TiO_2 в состояниях инвариантных равновесий. *Известия вузов. Черная металлургия*. 2004;47(6):7–11.
16. *Schlackenatlas*. Verein Deutscher Eisenhüttenleute, Verlag Stahleisen; 1981:282. (In Germ.).

    Атлас шлаков / Перевод с нем. Г.И. Жмойдина / Под ред. И.С. Куликова. Москва: Металлургия; 1985:208.
17. Nikolaychuk P.A. Thermodynamic evaluation of electrochemical stability of Me – Si systems (Me = 4th row transition metal). *Journal of Siberian Federal University. Chemistry*. 2015;8(2):160–180. https://doi.org/10.17516/1998-2836-2015-8-2-160-180
18. Bertoli A.C., Garcia J.S., Trevisan M.G., Ramalho T.C., Freitas M.P. Interactions fulvate-metal (Zn^{2+}, Cu^{2+} and Fe^{2+}): theoretical investigation of thermodynamic, structural and spectroscopic properties. *Biometals*. 2016;29:275–285. https://doi.org/10.1007/s10534-016-9914-8
19. Prostakova V., Shishin D., Shevchenko M., Jak E. Termodynamic optimization of the Al_2O_3 – FeO – Fe_2O_3 – SiO_2 oxide system. *Calphad*. 2019;67:101680. https://doi.org/10.1016/j.calphad.2019.101680

20. Sokol'skii V.E., Galinich V.I., Kazimirov V.P., Batalin G.I., Shovskii V.A. Structure of the molten ternary silicate systems $MnO–TiO_2–SiO_2$ and $MnO–ZrO_2–SiO_2$. *Melts*. 1989;1(6): 513–519.

Information about the Authors

***Nikolai F. Yakushevich*,** *Dr. Sci. (Eng.), Prof.-Consultant of the Chair of Non-Ferrous Metals and Chemical Engineering,* Siberian State Industrial University
E-mail: Yakushevich@cmet.sibsiu

***Evgenii V. Protopopov*,** *Dr. Sci. (Eng.), Prof. of the Chair of Ferrous Metallurgy,* Siberian State Industrial University
ORCID: 0000-0002-7554-2168
E-mail: protopopov@sibsiu.ru

***Mikhail V. Temlyantsev*,** *Dr. Sci. (Eng.), Prof., Vice-Rector for Educational and Tutorial Work,* Siberian State Industrial University
ORCID: 0000-0001-7985-5666
E-mail: uchebn_otdel@sibsiu.ru

***Irina V. Strokina*,** *Cand. Sci. (Eng.), Senior Lecturer of the Chair of Non-Ferrous Metals and Chemical Engineering,* Siberian State Industrial University
ORCID: 0000-0003-3719-8949
E-mail: chuzhinova.iv@yandex.ru

Сведения об авторах

***Николай Филиппович Якушевич*,** *д.т.н., профессор-консультант кафедры металлургии цветных металлов и химической технологии,* Сибирский государственный индустриальный университет
E-mail: Yakushevich@cmet.sibsiu

***Евгений Валентинович Протопопов*,** *д.т.н., профессор кафедры металлургии черных металлов,* Сибирский государственный индустриальный университет
ORCID: 0000-0002-7554-2168
E-mail: protopopov@sibsiu.ru

***Михаил Викторович Темлянцев*,** *д.т.н., профессор, проректор по учебной и воспитательной работе,* Сибирский государственный индустриальный университет
ORCID: 0000-0001-7985-5666
E-mail: uchebn_otdel@sibsiu.ru

***Ирина Владимировна Строкина*,** *к.т.н., старший преподаватель кафедры металлургии цветных металлов и химической технологии,* Сибирский государственный индустриальный университет
ORCID: 0000-0003-3719-8949
E-mail: chuzhinova.iv@yandex.ru

Contribution of the Authors

N. F. Yakushevich – statement of the task, analysis of literary data, complex thermodynamic analysis of co-reduction Zn and Fe by carbon, writing the text.

E. V. Protopopov – analysis of selected data to calculate the thermodynamic parameters of co-reduction of zinc and iron by carbon.

M. V. Temlyantsev – statement of the task, calculation of thermodynamic parameters of co-reduction of Zn and Fe by carbon, analysis of literary data, processing of the results, editing the final versions of the article.
I. V. Strokina – calculation of thermodynamic parameters of co-reduction of Zn and Fe by carbon, obtaining results, preparing drawings and tables.

Вклад авторов

Н. Ф. Якушевич – постановка задачи, анализ литературных источников, проведение комплексного термодинамического анализа процесса совместного восстановления цинка и железа углеродом, написание текста статьи.
Е. В. Протопопов – проведение анализа подобранных источников информации для расчета термодинамических параметров процесса совместного восстановления цинка и железа углеродом.
М. В. Темлянцев – постановка задачи, расчет термодинамических параметров совместного восстановления цинка и железа углеродом, анализ литературных источников, обработка результатов, редактирование финальной версии статьи.
И. В. Строкина – проведение расчетов термодинамических параметров процесса совместного восстановления цинка и железа углеродом, получение результатов, подготовка рисунков и таблицы для статьи.

Received 14.04.2022
Revised 15.03.2023
Accepted 20.03.2023

Поступила в редакцию 14.04.2022
После доработки 15.03.2023
Принята к публикации 20.03.2023